

Mutated hilltop inflation revisited

Barun Kumar Pal^a

^aDepartment of Mathematics
Netaji Nagar College for Women, Kolkata 700 092, INDIA

E-mail: terminatorbarun@gmail.com

Abstract. In this work we re-investigate pros and cons of mutated hilltop inflation. Applying Hamilton-Jacobi formalism we solve inflationary dynamics and find that inflation goes on along the \mathcal{W}_{-1} branch of the Lambert function. Depending on the model parameter mutated hilltop model renders two types of inflationary solution: one corresponds to small inflaton excursion during observable inflation and the other describes large field inflation. The inflationary observables from curvature perturbation are in tune with the current data for a wide range of the model parameter, $0 < \alpha M_{\text{P}} \leq \sqrt{11 + 5\sqrt{5}}$. The small field branch predicts negligible amount of tensor to scalar ratio $r \sim \mathcal{O}(10^{-4})$, while the large field sector is capable of generating high amplitude for tensor perturbations, $r \sim \mathcal{O}(10^{-1})$. Further we see that the spectral index is almost independent of the model parameter along with a very small negative amount of scalar running.

Contents

1	Introduction	1
2	Quick Look at Hamilton Jacobi Formalism	2
3	Mutated Hilltop Inflation: The Model	3
3.1	End of Inflation	4
3.2	Number of e-foldings	5
3.3	The Lyth Bound for MHI	6
3.4	Inflationary Observables in the Slow-Roll Limit	8
4	Conclusion	10

1 Introduction

The standard model of hot Big-Bang scenario is instrumental in explaining the nucleosynthesis, expanding universe along with the formation of cosmic microwave background (CMB henceforth). But there are few limitations in the likes of *flatness problem*, *homogeneity problem* etc., which can not be answered within the limit of Big-Bang cosmology. In order to overcome these shortcomings an early phase of accelerated expansion – *cosmic inflation* was proposed [1–3]. Big-Bang theory is incomplete without inflation and turns into brawny when combined with the paradigm of inflation. Though inflation was initiated to solve the cosmological puzzles, but the most impressive impact of inflation happens to be its ability to provide persuasive mechanism for the origin of cosmological fluctuations observed in the large scale structure and CMB. Nowadays inflation is the best bet for the origin of primordial perturbations.

Since its inception, almost four decades ago, inflation has remained the most powerful tool to explain the early universe when combined with big-bang scenario. It is still a paradigm due to the elusive nature of the scalar field(s), *inflaton*, responsible for inflation and the unknown shape of the potential involved. That the potential should be sufficiently flat to render almost scale invariant curvature perturbation [4, 5] has been only understood so far. As a result there are many inflationary models in the literature. With the advent of highly precise observational data from various probes [6–9], the window has become thinner, but still allowing numerous models to pass through [10, 11]. The recent detection of astronomical gravity waves by LIGO [12, 13] has made the grudging cosmologists waiting for primordial gravity waves which are believed to be produced during inflation through tensor perturbation. The upcoming stage-IV CMB experiments are expected to constrain the inflationary models further [14] by detecting primordial gravity waves.

The most efficient method for studying inflation is the slow-roll approximation [15], where the kinetic energy is assumed to be very small compared to the potential energy. But this is not the only way for successful implementation of inflation

and solutions outside slow-roll approximation have been found [16]. In order to study inflationary paradigm irrespective of slow-roll approximation Hamilton-Jacobi formalism [17, 18] has turned out to be very handy. Here the inflaton itself is treated as the evolution parameter instead of time, and the Friedmann equation becomes first order which is easy to extract underlying physics from.

Here we would like to study single field mutated hilltop model (MHI henceforth) of inflation [19, 20] using Hamilton-Jacobi formalism. In MHI observable inflation occurs as the scalar field rolls down towards the potential minimum. So MHI does not correspond to usual hilltop inflation [21, 22] directly, but the shape of the inflaton potential is somewhat similar to the mutated hilltop in hybrid inflation and hence the name. We shall see that for a wide range of values of the model parameter MHI provides inflationary solution consistent with recent observations. Our analysis also reveals that MHI has two different branches of inflationary solutions: one corresponds to small field inflation and the other represents large field inflation. In earlier studies [19, 20] we have reported that MHI can only produce a negligible amount of tensor to scalar ratio, $r \sim 10^{-4}$. But, we shall see here that it is capable of generating r as large as $\mathcal{O}(10^{-1})$ depending on the model parameter. Consequently a wide range of r , $10^{-4} \leq r \leq 10^{-1}$, can be addressed by MHI. Recent data from Planck [8, 9] has reported an upper bound $r_{0.002} < 0.1$ and upcoming CMB-S4 experiments are expected to survey tensor to scalar ratio up to $r \sim 2 \times 10^{-3}$ [14]. So sooner or later the model can be tested with the observations. The prediction for inflationary observables from MHI are in very good agreement with recent observational bound. Further, MHI predicts spectral index which is almost independent of model parameter along with small negative scalar running consistent with current data.

In Section 2 we have briefly reviewed Hamilton-Jacobi formalism. In the next Section 3 we have discussed about the MHI in Hamilton-Jacobi formalism. Finally we conclude in Section 4.

2 Quick Look at Hamilton Jacobi Formalism

The Hamilton-Jacobi formalism allows us to recast the Friedmann equation into the following form [16–18, 23]

$$\left[H'(\phi)\right]^2 - \frac{3}{2M_{\text{P}}^2}H(\phi)^2 = -\frac{1}{2M_{\text{P}}^4}V(\phi) \quad (2.1)$$

$$\dot{\phi} = -2M_{\text{P}}^2H'(\phi) \quad (2.2)$$

where prime and dot denote derivatives with respect to the scalar field ϕ and time respectively, and $M_{\text{P}} \equiv \frac{1}{\sqrt{8\pi G}}$ is the reduced Planck mass. The associated inflationary potential can then be found by rearranging the terms of Eqn.(2.1)

$$V(\phi) = 3M_{\text{P}}^2H^2(\phi) \left[1 - \frac{1}{3}\epsilon_{\text{H}}\right] \quad (2.3)$$

where ϵ_H has been defined as

$$\epsilon_H = 2M_P^2 \left(\frac{H'(\phi)}{H(\phi)} \right)^2. \quad (2.4)$$

We further have

$$\frac{\ddot{a}}{a} = H(\phi)^2 [1 - \epsilon_H]. \quad (2.5)$$

Therefore accelerated expansion takes place when $\epsilon_H < 1$ and ends exactly at $\epsilon_H = 1$. The evolution of the scale factor turns out to be

$$a \propto \exp \left[\int \frac{H}{\dot{\phi}} d\phi \right]. \quad (2.6)$$

The amount of inflation is expressed in terms of number of e-foldings and defined as

$$N \equiv \ln \frac{a_{\text{end}}}{a} = \frac{1}{M_P} \int_{\phi_{\text{end}}}^{\phi} \frac{1}{\sqrt{2\epsilon_H}} d\phi. \quad (2.7)$$

We have defined N in such a way that at the end of inflation $N = 0$ and N increases as we go back in time. The observable parameters are generally evaluated when there are 55 – 65 e-foldings still left before the end of inflation. It is customary to define another parameter by

$$\eta_H = 2M_P^2 \frac{H''(\phi)}{H(\phi)}. \quad (2.8)$$

It is worthwhile to mention here that the parameters ϵ_H and η_H are not the usual slow-roll parameters. But in the slow-roll limit $\epsilon_H \rightarrow \epsilon$ and $\eta_H \rightarrow \eta - \epsilon$ [15], ϵ and η being usual *potential slow-roll* parameters.

3 Mutated Hilltop Inflation: The Model

The potential we would like to study has the following form [19, 20]

$$V(\phi) = V_0 [1 - \text{sech}(\alpha\phi)] \quad (3.1)$$

where V_0 is the typical energy scale of inflation and α is a parameter having dimension of inverse Planck mass. The potential under consideration does not actually represent typical hilltop inflation [21, 22], but the form of the potential is somewhat similar to mutated hilltop inflation in hybrid scenario and hence the name. Accelerated expansion takes place as the inflaton rolls towards the potential minimum. Not only that, from Eq.(3.1) it is obvious that $V(\phi_{\text{min}}) = V'(\phi_{\text{min}}) = 0$ which is significantly different from the usual hilltop potential.

The associated Hubble parameter may be written as

$$H(\phi) \simeq \sqrt{\frac{V_0}{3M_P^2}} [1 - \text{sech}(\alpha\phi)]^{\frac{1}{2}} \quad (3.2)$$

The value of the constants can be fixed from the conditions for successful inflation and the observational bounds.

3.1 End of Inflation

Two parameters ϵ_H and η_H in the Hamilton Jacobi formalism now take the form

$$\epsilon_H = \frac{M_P^2 \alpha^2 \operatorname{sech}^2(\alpha\phi) \tanh^2(\alpha\phi)}{2(1 - \operatorname{sech}(\alpha\phi))^2}, \quad \eta_H = -\frac{M_P^2 \alpha^2}{2} \operatorname{sech}(\alpha\phi) [2 + 3 \operatorname{sech}(\alpha\phi)] \quad (3.3)$$

The inflation ends naturally when $\epsilon_H = 1$ at ϕ_{end} , which is the root of the following equation

$$M_P^2 \alpha^2 \operatorname{sech}^2(\alpha\phi_{\text{end}}) (1 - \operatorname{sech}^2(\alpha\phi_{\text{end}})) = 2(1 - \operatorname{sech}(\alpha\phi_{\text{end}}))^2. \quad (3.4)$$

Eq.(3.4) can be solved analytically and the relevant solution turns out to be

$$\begin{aligned} \phi_{\text{end}} = M_P b^{-1} \operatorname{sech}^{-1} \frac{1}{3} \left[-1 + \frac{b^2 - 6}{b(36b - b^3 + 3\sqrt{6}\sqrt{4 + 22b^2 - b^4})^{1/3}} \right. \\ \left. + \frac{(36b - b^3 + 3\sqrt{6}\sqrt{4 + 22b^2 - b^4})^{1/3}}{b} \right] \end{aligned} \quad (3.5)$$

where $b \equiv \alpha M_P$. On the other hand absolute value of η_H becomes order of unity at

$$\phi = \alpha^{-1} \operatorname{sech}^{-1} \frac{1}{3} \left[-1 + \sqrt{1 + \frac{6}{b^2}} \right]. \quad (3.6)$$

In Fig.1 we have shown the variation of the ϕ_{end} with α and the solution of $|\eta_H(\phi)| = 1$. From the figure it is obvious that the $|\eta_H| = 1$ occurs well before the actual end of inflation for $\alpha \geq \alpha_{\text{eq}}$, where α_{eq} represents the value of α for the simultaneous occurrence of $|\eta_H| = 1$ and $\epsilon_H = 1$, which can be found analytically from Eq.(3.5) and Eq.(3.6), $\alpha_{\text{eq}} = 2\sqrt{3 - 2\sqrt{2}} M_P^{-1}$ and corresponding value of the inflaton is given by $\alpha_{\text{eq}}^{-1} \operatorname{sech}^{-1} \left(\frac{1}{\sqrt{2}} \right)$. Consequently, slow-roll approximation becomes poor towards the end of inflation for $\alpha \geq \alpha_{\text{eq}}$. But this is not so problematic as we are interested at the value of inflaton when cosmologically relevant scales leave the horizon and there slow-roll is a very good approximation. Also this happens only for negligible period of time as shown in Fig.2. On the other hand for $\alpha < \alpha_{\text{eq}}$ the situation is somewhat different, $\epsilon_H = 1$ precedes $|\eta_H| = 1$. Here we would like to mention that for $\alpha < \sqrt{\frac{2}{5}} M_P^{-1}$, $|\eta_H|$ always remains below the unity. Therefore slow-roll approximation is valid till the end of inflation. It is possible to derive a bound on the model parameter α , by demanding that inflation ends through the violation of the slow-roll approximation and for that we need ϕ_{end} to be a real number. Imposing that restriction we find $0 < \alpha M_P \leq \sqrt{11 + 5\sqrt{5}}$. For the rest of the article we shall adhere to this range of α only.

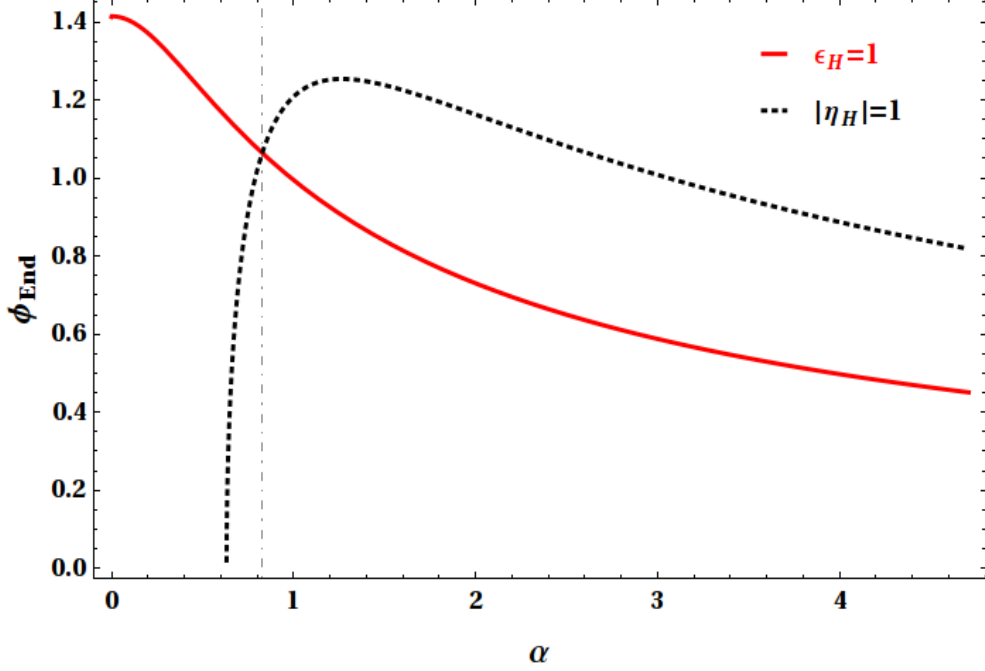


Figure 1. The solid line is the variation of ϕ_{end} with the model parameter α and the dotted line represents the variation of scalar field for which $|\eta_H| = 1$ with α . The dashed vertical line represents the value of α for the simultaneous occurrence of $\eta_H = 1$ and $|\eta_H| = 1$.

3.2 Number of e-foldings

The number of e-foldings for MHI is found to have the following form

$$N(\phi) = \frac{1}{\alpha^2 M_{\text{P}}^2} \left[\cosh(\alpha\phi) - \cosh(\alpha\phi_{\text{end}}) - 2 \ln \frac{\cosh(\alpha\phi/2)}{\cosh(\alpha\phi_{\text{end}}/2)} \right]. \quad (3.7)$$

The above Eq.(3.7) can be analytically inverted to get the scalar field as a function of e-foldings as follows

$$\begin{aligned} \phi &= \alpha^{-1} \cosh^{-1} \left[-1 - \mathcal{W}_{-1} \left(-[\cosh(\alpha\phi_{\text{end}}) + 1] e^{-M_{\text{P}}^2 \alpha^2 N - 1 - \cosh(\alpha\phi_{\text{end}})} \right) \right] \\ &= \alpha^{-1} \cosh^{-1} \left[-1 - \mathcal{W}_{-1} \left(-[M_{\text{P}} \phi_{\text{end}}^{-1} + 1] e^{-M_{\text{P}}^2 \alpha^2 N - 1 - M_{\text{P}} \phi_{\text{end}}^{-1}} \right) \right] \\ &= \alpha^{-1} \cosh^{-1} (\mathcal{LW}[\alpha, N]) \end{aligned} \quad (3.8)$$

where we have defined $\mathcal{LW}[\alpha, N] \equiv \left[-1 - \mathcal{W}_{-1} \left(-[M_{\text{P}} \phi_{\text{end}}^{-1} + 1] e^{-M_{\text{P}}^2 \alpha^2 N - 1 - M_{\text{P}} \phi_{\text{end}}^{-1}} \right) \right]$ and \mathcal{W}_{-1} is the Lambert function. From the above Eq.(3.8), one can see that mutated hilltop inflation occurs along the \mathcal{W}_{-1} branch of the Lambert function, first pointed out in Ref.[10]. The value of the inflaton when cosmological scale leaves the horizon, ϕ_{CMB} , is then given by

$$\phi_{\text{CMB}} = \alpha^{-1} \cosh^{-1} (\mathcal{LW}[\alpha, N_{\text{CMB}}]) \quad (3.9)$$

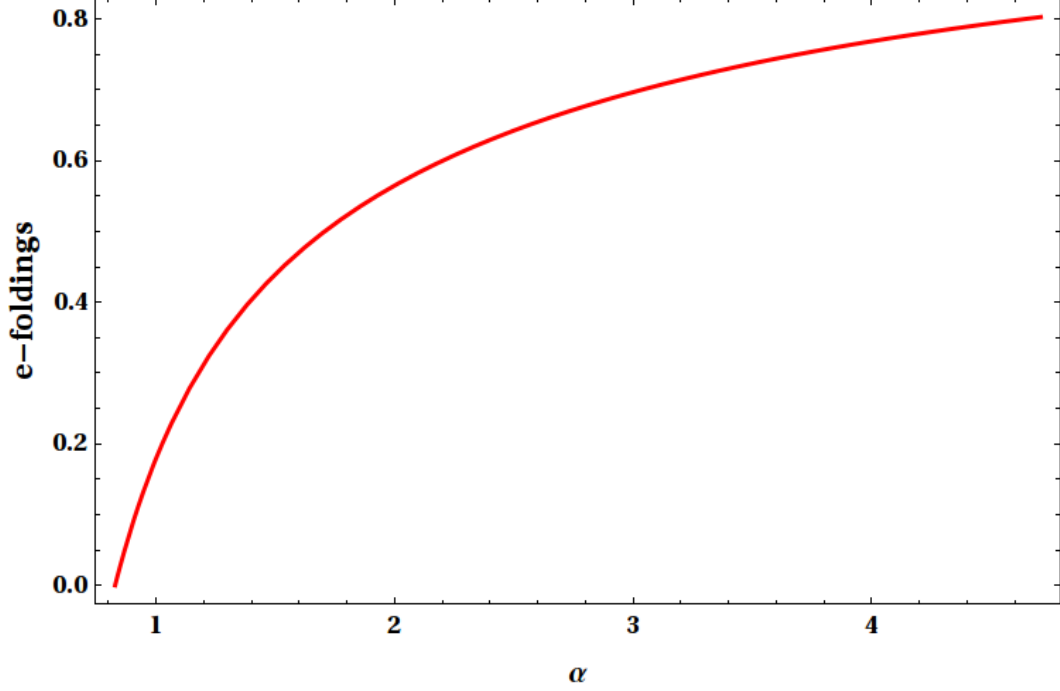


Figure 2. No. of e-folding required by the scalar field to evolve from $|\eta_H| = 1$ to $\epsilon_H = 1$ for $\alpha \geq \alpha_{\text{eq}}$ in MHI.

The slow-roll parameters now can be expressed as a function of the e-foldings

$$\begin{aligned}\epsilon_H &= \frac{1}{2M_{\text{P}}^2} \left(\frac{d\phi}{dN} \right)^2 \\ &= \frac{M_{\text{P}}^2 \alpha^2}{2} \frac{\mathcal{LW}[\alpha, N] + 1}{(\mathcal{LW}[\alpha, N] - 1) \mathcal{LW}[\alpha, N]^2}\end{aligned}\quad (3.10)$$

$$\begin{aligned}\eta_H &= \left(\frac{d^2\phi}{dN^2} \right) \left(\frac{d\phi}{dN} \right)^{-1} + \epsilon_H \\ &= -\frac{M_{\text{P}}^2 \alpha^2}{2} \frac{2\mathcal{LW}[\alpha, N] + 3}{\mathcal{LW}[\alpha, N]^2}\end{aligned}\quad (3.11)$$

This makes life simpler as now all the inflationary observable parameters when derived in the slow-roll limit can be expressed as a function of N .

3.3 The Lyth Bound for MHI

The fluctuations in the tensor modes solely depends on the Hubble parameter whereas curvature perturbation is a function of the Hubble parameter and inflaton. Consequently, tensor to scalar ratio determines excursion of the inflaton during observable inflation, first shown in Ref.[24] and known as Lyth bound

$$\Delta\phi = \frac{m_{\text{P}}}{8\sqrt{\pi}} \int_0^{N_{\text{CMB}}} \sqrt{r} \, dN \quad (3.12)$$

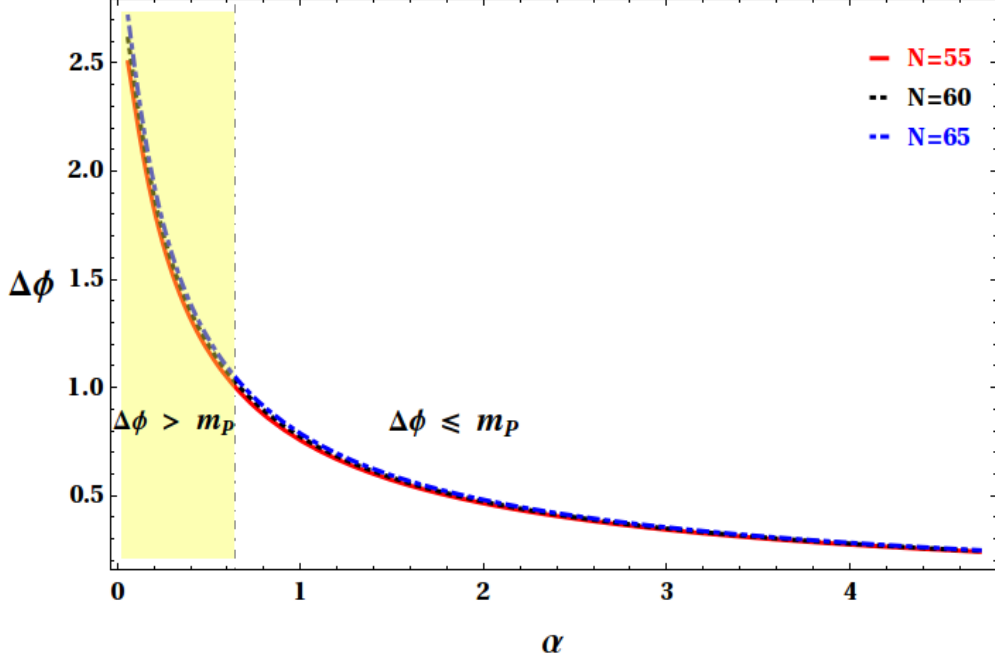


Figure 3. Excursion of the scalar field (in the unit of m_P) with the model parameter α for three different values of e-foldings, $N = 55, 60, 65$. The dotted vertical line corresponds to the value of α at which $\Delta\phi = m_P$ which has been estimated by considering $N_{\text{CMB}} = 55$.

where $m_P = 2\sqrt{2\pi}M_P$ is the actual Planck mass. $\Delta\phi \geq m_P$ corresponds to large field model and $\Delta\phi < m_P$ small field models. One expects to get larger tensor to scalar ratio, r , where $\Delta\phi \geq m_P$ due to the higher energy scale required for successfully explaining the observable parameters.

For the model under consideration we have found

$$\Delta\phi = \alpha^{-1} \cosh^{-1}(\mathcal{LW}[\alpha, N_{\text{CMB}}]) - \alpha^{-1} \cosh^{-1}(\mathcal{LW}[\alpha, 0]) \quad (3.13)$$

In Fig.3 we have shown the variation of the scalar field excursion in the unit of m_P , with the model parameter α . From the figure it is obvious that the mutated hilltop model of inflation has small excursion of the inflaton for $\alpha \geq \alpha_{\Delta\phi=1}$ and large field excursion for $\alpha < \alpha_{\Delta\phi=1}$, where $\alpha_{\Delta\phi=1}$ is the solution of Eq.(3.13) for α with $\Delta\phi = m_P$. So this model is capable of addressing both the large and small field inflationary scenarios for suitable values of the model parameter. In Fig.4 we have shown the variation of $\text{Log}_{10}r$ with $\Delta\phi$. From the figure we see that small field MHI may give rise to negligible amount of tensor to scalar ratio, $r \sim \mathcal{O}(10^{-4})$, on the other hand for large $\Delta\phi$, r can be as large as $\mathcal{O}(10^{-1})$.

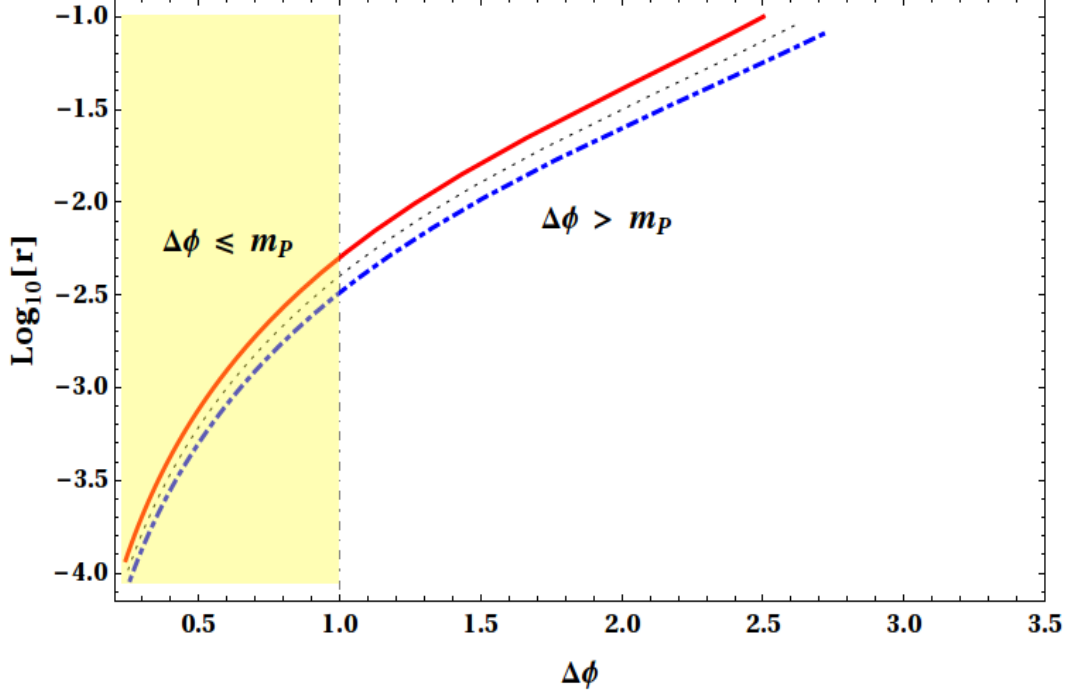


Figure 4. The logarithmic variation of the tensor to scalar ratio with $\Delta\phi$ for three values of N_{CMB} has been plotted. Red solid line for $N_{\text{CMB}} = 55$, black dotted curve represents $N_{\text{CMB}} = 60$ and the blue dashed line for $N_{\text{CMB}} = 65$.

3.4 Inflationary Observables in the Slow-Roll Limit

The inflationary observable parameters can be found analytically in the slow-roll approximation. The power spectrum of the curvature perturbation turns out to be

$$\begin{aligned}
 P_{\mathcal{R}} &\simeq \frac{1}{16\pi^2 M_{\text{P}}^4} \left[\frac{H(\phi)^2}{H'(\phi)} \right]_{\phi=\phi_{\text{CMB}}}^2 \\
 &= \frac{V_0}{12\pi^2 \alpha^2 M_{\text{P}}^6} \frac{\mathcal{LW}[\alpha, N_{\text{CMB}}] (\mathcal{LW}[\alpha, N_{\text{CMB}}] - 1)^2}{\mathcal{LW}[\alpha, N_{\text{CMB}}] + 1}
 \end{aligned} \tag{3.14}$$

In Fig.5 we have shown the variation of the typical energy scale associated with MHI for different values of the model parameter. From the figure it is clear that maximum energy scale that can be achieved is $\mathcal{O}(10^{16})$ GeV. To determine this energy scale we have used $P_{\mathcal{R}} = 2.142 \times 10^{-9}$ from Planck 2015 result [9]. The scale dependence of the spectrum of curvature perturbation is described by spectral index. In MHI we have found

$$\begin{aligned}
 n_S &\simeq 1 - 4\epsilon_H|_{\phi=\phi_{\text{CMB}}} + 2\eta_H|_{\phi=\phi_{\text{CMB}}} \\
 &= 1 - M_{\text{P}}^2 \alpha^2 \frac{2\mathcal{LW}[\alpha, N_{\text{CMB}}]^2 + 3\mathcal{LW}[\alpha, N_{\text{CMB}}] - 1}{\mathcal{LW}[\alpha, N_{\text{CMB}}]^2 (\mathcal{LW}[\alpha, N_{\text{CMB}}] - 1)}
 \end{aligned} \tag{3.15}$$

In Fig.6 we have shown how the scalar spectral index changes with the model param-

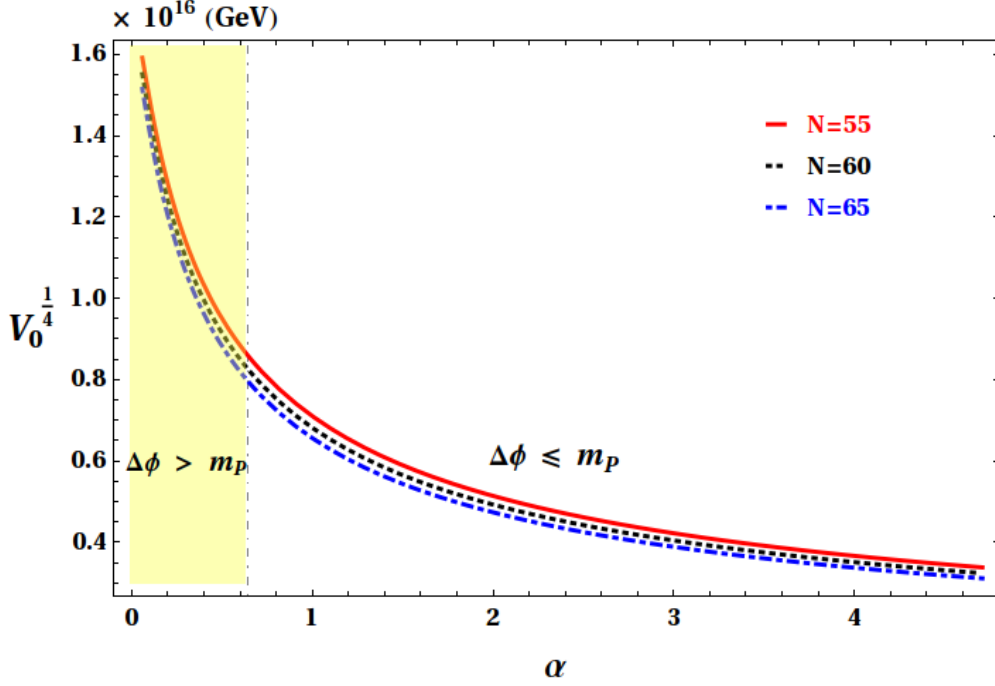


Figure 5. The energy scale in the unit of GeV for MHI has been plotted with the model parameter α for $N_{\text{CMB}} = 55, 60, 65$. The shaded region corresponds to the large field sector for MHI.

eter. We also see that spectral index is almost constant in both the large and small field sector of MHI. The current bound on n_s from Planck 2015 has also been shown.

The scale dependence of the spectral index itself is estimated from the scalar running and we have

$$\begin{aligned}
 n'_s &\simeq -2M_{\text{P}}^4 H'(\phi)H'''(\phi)/H^2(\phi)|_{\phi=\phi_{\text{CMB}}} + 16\epsilon_H\eta_H|_{\phi=\phi_{\text{CMB}}} - 8\epsilon_H^2|_{\phi=\phi_{\text{CMB}}} \\
 &= -\frac{M_{\text{P}}^4\alpha^4}{2} [-32 + 30\mathcal{LW}[\alpha, N_{\text{CMB}}] + 33 \cosh(2 \cosh^{-1} \mathcal{LW}[\alpha, N_{\text{CMB}}]) \\
 &\quad + \cosh(3 \cosh^{-1} \mathcal{LW}[\alpha, N_{\text{CMB}}])] \mathcal{LW}[\alpha, N_{\text{CMB}}]^{-4} (\mathcal{LW}[\alpha, N_{\text{CMB}}] + 1)^{-1} \\
 &\quad \times (\mathcal{LW}[\alpha, N_{\text{CMB}}] - 1)^{-2}
 \end{aligned} \tag{3.16}$$

Here in Fig.7 logarithmic variation of the absolute value of scalar running with α has been plotted. From the figure it is clear that MHI predicts very small running of the spectral index. The maximum amount of scalar running that can achieved in MHI is $|n'_s| \sim 10^{-3}$.

Finally, the tensor to scalar ratio is found to have the following form

$$\begin{aligned}
 r &\simeq 16\epsilon_H|_{\phi=\phi_{\text{CMB}}} \\
 &= 8M_{\text{P}}^2\alpha^2 \frac{\mathcal{LW}[\alpha, N_{\text{CMB}}] + 1}{\mathcal{LW}[\alpha, N_{\text{CMB}}]^2 (\mathcal{LW}[\alpha, N_{\text{CMB}}] - 1)}
 \end{aligned} \tag{3.17}$$

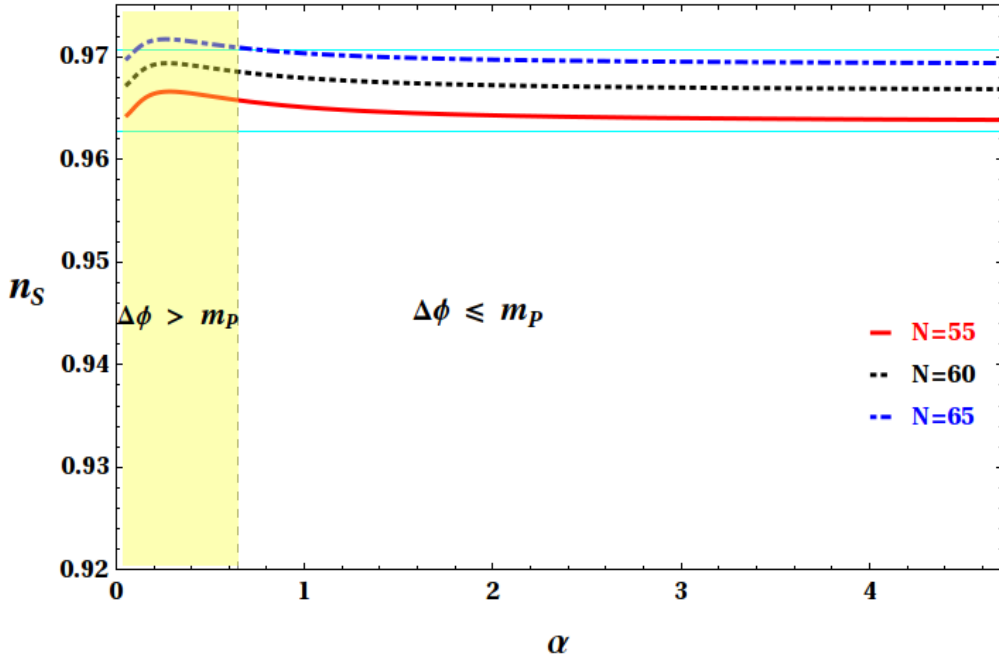


Figure 6. The variation of the scalar spectral index with α for three different values of N_{CMB} has been plotted. The shaded vertical region is the result for large field sector of MHI. The two horizontal lines (cyan) are for Planck 2015 upper & lower bound on n_s .

In Fig.8 we have plotted the tensor to scalar ratio (in Log_{10} scale) with α for three different values of N_{CMB} . We see that MHI can address wide range of values of tensor to scalar ratio, $10^{-4} \leq r \leq 10^{-1}$ depending on the model parameter α . But $r \sim 10^{-1}$ has to be discarded which is observationally forbidden which determines a lower bound on the model parameters, $\alpha > 0.05855$.

In Fig.9 we exhibit variation of the MHI energy scale with the tensor to scalar ratio. So in order to achieve $r \sim 10^{-1}$ we need an energy scale $V_0^{\frac{1}{4}} \sim 1.6 \times 10^{16}$ GeV.

4 Conclusion

In this article we have revisited mutated hilltop inflation driven by a hyperbolic potential. Employing Hamilton-Jacobi formulation we found that inflation ends naturally through the violation slow-roll approximation. More interestingly, MHI has two different branches of inflationary solution. One corresponds to large field variation and the other represents small change in inflaton during the observable inflation depending on the model parameter.

Observable parameters as derived from this model are in tune with the latest observations for a wide range of the model parameter, $0.05855 < \alpha M_{\text{P}} \leq \sqrt{11 + 5\sqrt{5}}$. The scalar spectral index is found to be independent of the model parameter with a small negative running. We have also found that MHI can address a broad range of the

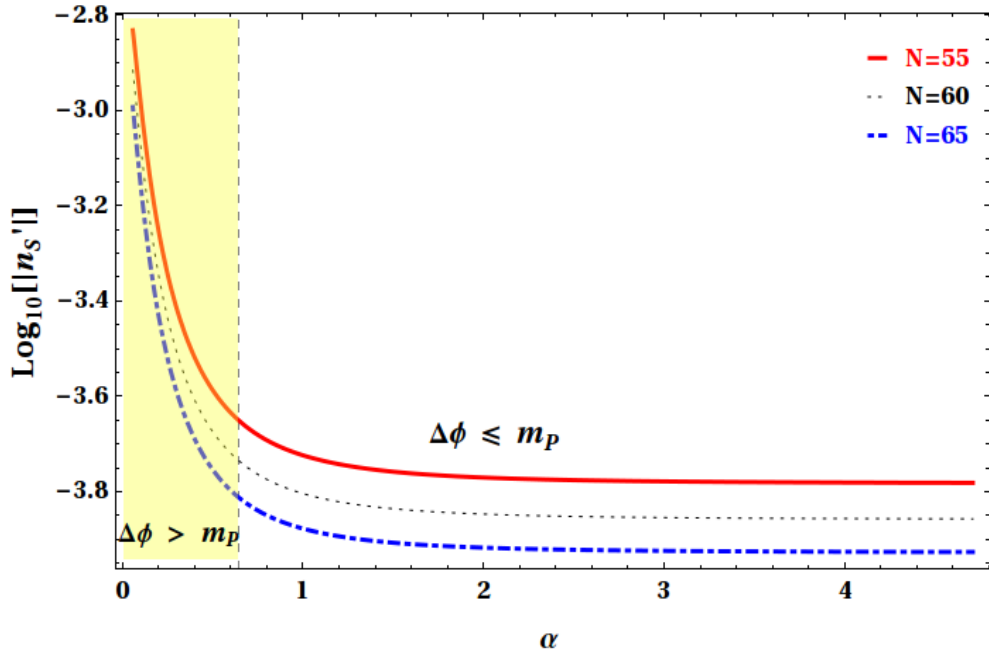


Figure 7. The logarithmic variation of the absolute value of the scalar running with α for three different values of N_{CMB} has been plotted. The shaded vertical region is the result for large field sector of the model under consideration.

tensor to scalar ratio, $0.0001 \leq r \leq 0.1$. In a nutshell, MHI though does not belong to the usual hilltop inflation is extremely attractive with only one model parameter consistent with recent observations.

Acknowledgment

I would like to thank Supratik Pal for useful discussions and constructive suggestions. I would also like to thank IUCAA, Pune for giving me the opportunity to carry on research work through their Associateship Program.

References

- [1] A. H. Guth. [The Inflationary Universe: A Possible Solution to the Horizon and Flatness Problems](#). *PRD*, **23**: 247, 1981.
- [2] A. Albrecht and P. J. Steinhardt. [Cosmology for grand unified theories with radiatively induced symmetry breaking](#). *PRL*, **48**: 1220, 1982.
- [3] A. D. Linde. [A new inflationary universe scenario: s possible solution of the horizon, flatness, homogeneity, isotropy and pimordial monopole problems](#). *PLB*, **108**: 389, 1982.
- [4] Viatcheslav F. Mukhanov, H. A. Feldman, and Robert H. Brandenberger. [Theory of cosmological perturbations](#). *Phys. Rept.*, **215**: 203, 1992.

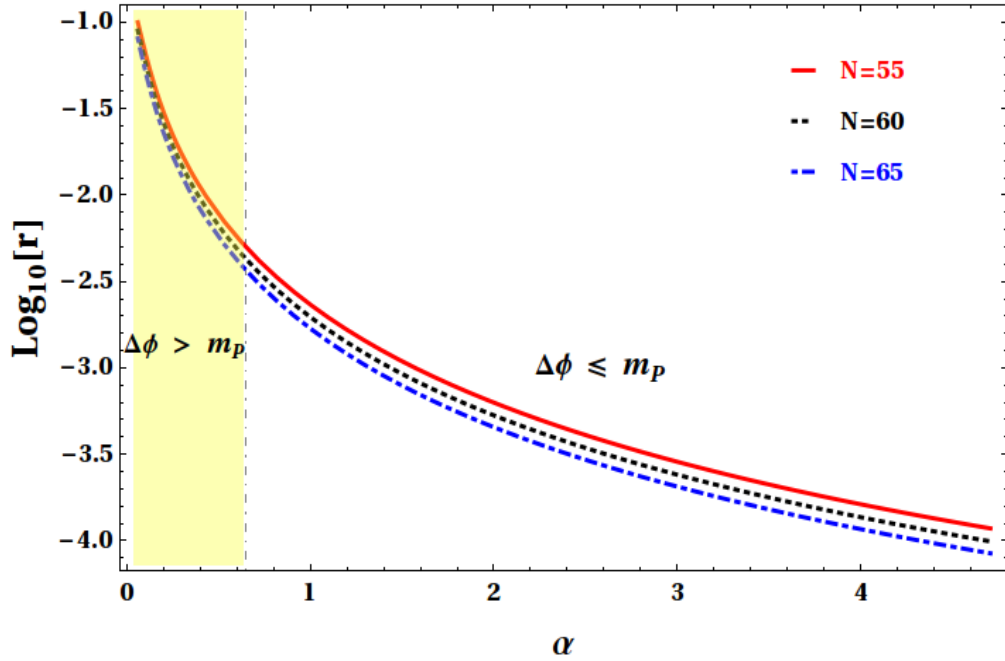


Figure 8. Logarithmic variation of the tensor to scalar ratio with α for three different values of N_{CMB} has been plotted. The shaded vertical region corresponds to the large field sector of the MHI.

- [5] E. D. Stewart and D. H. Lyth. [A more accurate analytic calculation of the spectrum of cosmological perturbations produced during inflation](#). *PLB*, **302**: 171, 1993.
- [6] G. F. Smoot et al. [Structure in the COBE differential microwave radiometer first-year maps](#). *ApJ*, **396**: L1–L5, 1992.
- [7] G. Hinshaw et. al. [Nine-Year Wilkinson Microwave Anisotropy Probe \(WMAP\) Observations: Cosmological Parameter Results](#). *ApJ Supplement Series*, **208**:19, 2013.
- [8] P. A. R. Ade et al. [Planck 2015 results-XIII. Cosmological parameters](#). *A&A*, **594**:A13, 2016.
- [9] P. A. R. Ade et al. [Planck 2015 results-XX. Constraints on inflation](#). *A&A*, **594**:A20, 2016.
- [10] J. Martin, C. Ringeval, and V. Vennin. [Encyclopædia inflationaris](#). *Physics of the Dark Universe*, **5**: 75, 2014.
- [11] J. Martin, C. Ringeval, R. Trotta, and V. Vennin. [The best inflationary models after Planck](#). *JCAP*, **03**:039, 2014.
- [12] B. P. Abbott et al. [Observation of gravitational waves from a binary black hole merger](#). *PRL*, **116**:061102, 2016.
- [13] B. P. Abbott et al. [Observation of Gravitational Waves from a 22-Solar-Mass Binary Black Hole Coalescence](#). *PRL*, **116**:241103, 2016.
- [14] K. N. Abazajian et al. [CMB-S4 Science Book](#). *arXiv preprint arXiv:1610.02743*, 2016.

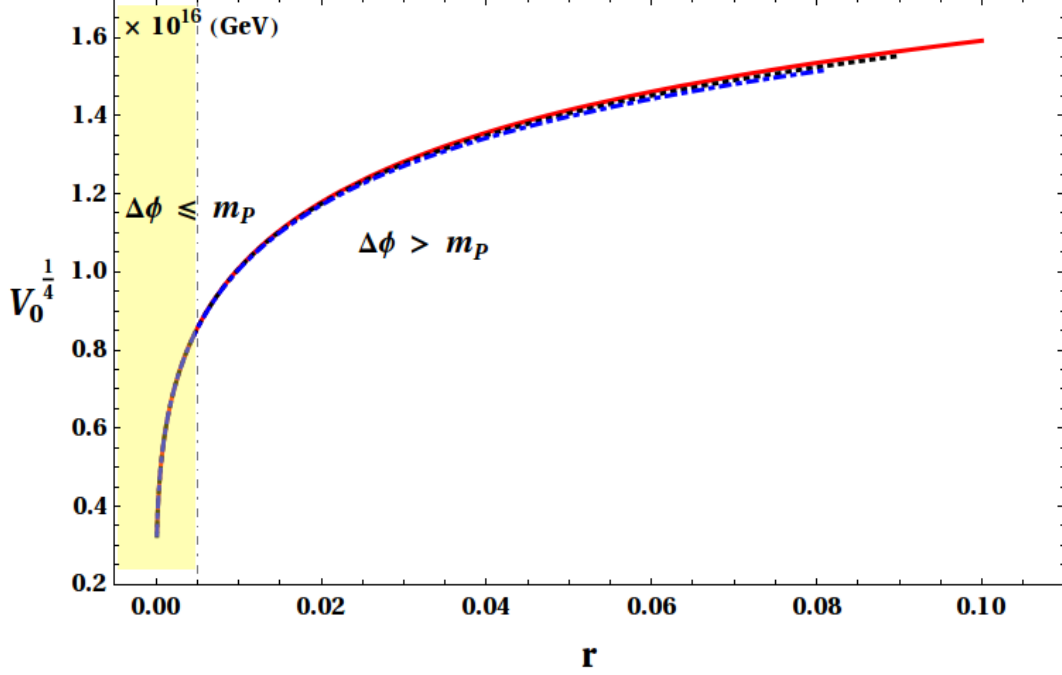


Figure 9. Variation of the MHI energy scale with r has been shown for three different values of N_{CMB} . Red solid line is for $N_{\text{CMB}} = 55$, black dotted curve represents $N_{\text{CMB}} = 60$ and the blue dashed line for $N_{\text{CMB}} = 65$. The shaded vertical region represents small field sector of MHI.

- [15] A. R. Liddle, P. Parsons, and J. D. Barrow. [Formalising the Slow-Roll Approximation in Inflation](#). *PRD*, **50**: 7222–7232, 1994.
- [16] W. Kinney. [Hamilton-Jacobi approach to non-slow-roll inflation](#). *PRD*, **56**: 2002–2009, 1997.
- [17] D. Salopek and J. Bond. [Nonlinear evolution of long wavelength metric fluctuations in inflationary models](#). *PRD*, **42**: 3936–3962, 1990.
- [18] A. Muslimov. [On the scalar field dynamics in a spatially flat Friedman universe](#). *CQG*, **7**: 231, 1990.
- [19] Barun Kumar Pal, Supratik Pal, and B. Basu. [Mutated hilltop inflation: a natural choice for early universe](#). *JCAP*, **01**: 029, 2010.
- [20] Barun Kumar Pal, Supratik Pal, and B. Basu. [A semi-analytical approach to perturbations in mutated hilltop inflation](#). *IJMPD*, **21**: 1250017, 2012.
- [21] L. Boubekeur and D. H. Lyth. [Hilltop inflation](#). *JCAP*, **07**: 010, 2005.
- [22] K. Kohri, C. M. Lin, and D. H. Lyth. [More hilltop inflation models](#). *JCAP*, **12**: 004, 2007.
- [23] Barun Kumar Pal, Supratik Pal, and B. Basu. [Confronting quasi-exponential inflation with WMAP seven](#). *JCAP*, **04**: 009, 2012.
- [24] D. H. Lyth. [What Would We Learn by Detecting a Gravitational Wave Signal in the Cosmic Microwave Background Anisotropy?](#) *PRL*, **78**: 1861, 1997.